PHYSICAL REVIEW D **88,** 015021 (2013)

Xenophobic dark matter

Jonathan L. Feng,[1,*] Jason Kumar,[2,†] and David Sanford[3,‡]

[1]*Department of Physics and Astronomy, University of California, Irvine, California 92697, USA*
[2]*Department of Physics and Astronomy, University of Hawaii, Honolulu, Hawaii 96822, USA*
[3]*Department of Physics, California Institute of Technology, Pasadena, California 91125, USA*

(Received 20 June 2013; published 15 July 2013)

We consider models of xenophobic dark matter, in which isospin-violating dark matter–nucleon interactions significantly degrade the response of xenon direct detection experiments. For models of near-maximal xenophobia, with neutron-to-proton coupling ratio $f_n/f_p \approx -0.64$, and dark matter mass near 8 GeV, the regions of interest for CoGeNT and CDMS-Si and the region of interest identified by Collar and Fields in CDMS-Ge data can be brought into agreement. This model may be tested in future direct, indirect, and collider searches. Interestingly, because the natural isotope abundance of xenon implies that xenophobia has its limits, we find that this xenophobic model may be probed in the near future by xenon experiments. Near-future data from the LHC and Fermi-LAT may also provide interesting alternative probes of xenophobic dark matter.

DOI: 10.1103/PhysRevD.88.015021 PACS numbers: 95.35.+d, 12.60.Jv

I. INTRODUCTION

In recent years experimental progress in direct detection of dark matter has been extraordinary, especially for dark matter that exhibits spin-independent (SI) nuclear scattering. Candidates with relatively low masses of $\sim$10 GeV have been particularly exciting, with potential signals at DAMA [1], CoGeNT [2], CRESST [3], and CDMS [4]. Although the tentative signals are generally within the same region of parameter space, they do not produce consistent determinations of either mass or interaction cross section given conventional assumptions. Moreover, several direct detection experiments have reported the absence of an excess of events, with XENON100 [5,6] placing particularly strong constraints on these results [see Fig. 1(a)]. This has led to recent attempts to reconcile the results of these experiments by considering theories that deviate from standard assumptions about dark matter interactions or its astrophysical distributions [7–9].

In this work, we focus on the possibility of isospin-violating dark matter (IVDM), in which dark matter interacts with protons and neutrons with different couplings [10–14]. IVDM is a highly motivated generalization of the conventional isospin-invariant case: weakly interacting massive particles (WIMPs) do not resolve the internal structure of nucleons, but they do resolve the nucleon structure within nuclei. Irrespective of attempts to explain or reconcile data, IVDM parametrizes the scattering off of matter in terms of the smallest structure WIMP scattering resolves. Indeed, in the spin-dependent direct detection literature, isospin-violating effects are generally considered. Although some well-known dark matter candidates, such as the neutralino in simple supersymmetric models, have effectively isospin-invariant interactions, this is not generically the case, as we detail below. In this data-rich era, it is appropriate to shed theoretical prejudices to the extent possible, and IVDM provides an extremely natural framework to analyze direct detection data.

A reanalysis of IVDM is motivated by several recent developments in direct detection experiments, including limits from the XENON10 [15] and XENON100 [5,6] experiments, new exclusion contours from a low-mass analysis of CDMS-Ge detectors [16,17], modifications to the CoGeNT region of interest (ROI) [18,19] due to greater exposure and a better understanding of surface event contamination, a new ROI arising from an excess of events seen by CRESST [3], and most recently a new ROI arising from an excess of events seen by the CDMS-Si detectors [4].

In light of these developments, this paper will revisit IVDM in the context of low-mass dark matter. The tightest constraints on low-mass dark matter arise from XENON100, so any attempt to reconcile the positive signals of some detectors with the negative signals from others must focus on *xenophobic dark matter*, in which the sensitivity of xenon-based detectors is highly suppressed by destructive interference between proton and neutron interactions. It is important to note [14] that the sensitivity of xenon-based detectors cannot be suppressed arbitrarily, given the significant abundances of multiple isotopes of xenon; no choice of relative couplings can completely cancel the response of all of xenon's isotopes simultaneously. For example, it does not appear possible to obtain consistency between XENON100 exclusion contours and either the DAMA or CRESST ROIs, even with maximally xenophobic dark matter. As a result, we will not focus on those experiments.

We will take as our guideposts the CoGeNT ROI found in Refs. [18,19] and the ROI found by Collar and Fields in an analysis of the recoil spectrum of all CDMS-Ge

*jlf@uci.edu
†jkumar@hawaii.edu
‡dsanford@caltech.edu

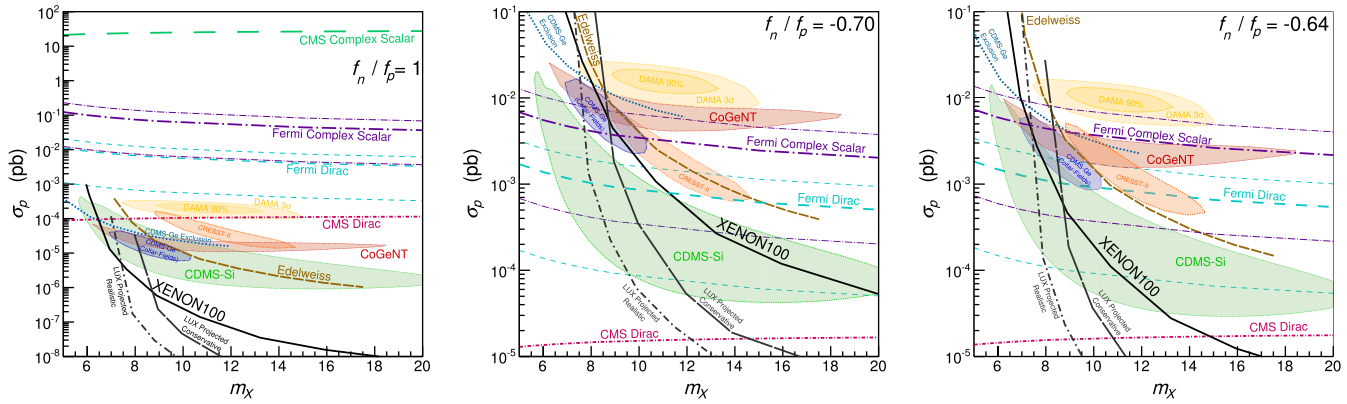

FIG. 1 (color online). Regions of interest and exclusion contours in the (m_X, σ_p) for neutron-to-proton coupling ratios $f_n/f_p = 1$ (left), $f_n/f_p = -0.70$ (center) and $f_n/f_p = -0.64$ (right). Plotted are the 90% CL ROIs for CDMS-Si [4], CoGeNT [2], and CDMS-Ge (Collar/Fields) [20], the 90% and 3σ ROIs for DAMA [1] as determined in Refs. [45,46], and exclusion contours from XENON100 [5,6], Edelweiss [47], and CDMS [17], and projected exclusion bounds from LUX [21]. Recent TEXONO [48] and CDEX-1 [49] bounds (not shown) are similar but moderately weaker than CDMS bounds over the mass interval shown. Also plotted are 90% CL exclusion contours from CMS and from the Fermi-LAT, assuming dark matter is either a complex scalar or Dirac fermion coupling only to first generation quarks through an effective contact interaction permitting unsuppressed spin-independent scattering and S-wave annihilation. The thin dot-dashed violet and dashed teal lines correspond to the systematic uncertainty in the Fermi-LAT bounds from astrophysical uncertainties for complex scalar and Dirac fermion candidates, respectively. In the center and right panels the CMS complex scalar exclusion bounds exceed the plotted range by between 1 and 2 orders of magnitude, and thus place no constraints on the disputed region.

detectors [20]. Although there have been several questions regarding the status of signals in germanium-based detectors, we will find it useful to treat these ROIs as benchmarks, because they identify a relatively small region of parameter space near $m_X \sim 8$ GeV in which the potential signals and exclusion contours of current germanium-based detectors can all be satisfied. Our focus will be on obtaining consistency of these regions with exclusion contours from xenon-based detectors, consistency with the CDMS-Si ROI, and ways of testing these models with near-future direct detection, indirect detection, and collider searches.

We will find that although maximally xenophobic dark matter with $f_n/f_p \simeq -0.70$ [Fig. 1(b)] reduces the tension between the germanium-based ROIs and the xenon-based exclusion contours, the germanium-based and silicon-based ROIs do not overlap. On the other hand, for near-maximally xenophobic dark matter with $f_n/f_p = -0.64$ [Fig. 1(c)], there is a region of parameter space where the germanium-based and silicon-based ROIs overlap, which is consistent with xenon-based 90% CL exclusion contours. This model may be decisively probed by the LUX experiment [21]. Moreover, we will see that xenophobic dark matter is much more amenable to indirect and collider detection strategies; some xenophobic models for the low-mass data can be excluded by current CMS monojet analyses, while other models will be tested soon with new Fermi-LAT data on gamma rays from dwarf spheroidal galaxies. More generally, we will see that, given any signals of dark matter at a direct detection experiment, it is necessary to compare the results of multiple experiments, including collider experiments and experiments using indirect detection strategies, to determine the dark matter-nucleon couplings.

In Sec. II we review the general nature of isospin-violating couplings and discuss the relationship between the normalized-to-nucleon cross section usually reported by experiments and the actual dark matter–proton scattering cross section. In Sec. III we focus on xenophobic dark matter. We conclude with a discussion of our results in Sec. IV.

II. GENERAL ISOSPIN-VIOLATING COUPLINGS

A. The case for isospin-violating interactions

Although isospin-invariant couplings are generally assumed when reporting direct detection results, isospin-violating couplings are in fact generic for theories with WIMPs. This results from the fact that interactions of WIMPs are typically related to electroweak symmetry and, in particular, to hypercharge. Since right-handed up and down quarks have different hypercharge, it would be natural to expect these interactions to depend on isospin. The fact that the spin-independent scattering matrix element is largely isospin invariant for WIMPs in some scenarios, such as the constrained minimal supersymmetric standard model (CMSSM), is actually the result of several nontrivial coincidences. For example, in the CMSSM, the Bino component of the lightest supersymmetric particle (LSP) can scatter off nuclei through squark exchange, and

this matrix element is generally isospin violating, but the spin-independent piece of the matrix element is proportional to the left-right squark-mixing angle. Under the assumption of minimal flavor violation (as in the CMSSM) this angle is small for first generation squarks. The Higgsino component can also scatter through Z-exchange, which again produces an isospin-violating contribution to the matrix element. But since the LSP is a Majorana fermion, the leading term is again spin dependent. The Wino/Higgsino component of the LSP can scatter off nuclei through Higgs exchange, and this contribution to the scattering matrix element is spin independent, but it is also largely isospin invariant because the coupling is proportional to the quark mass. The assumption of isospin-invariant interactions is really only justified within this narrow framework and others like it, and these frameworks can realize a low-mass dark matter candidate only with great difficulty.

Indeed, for many models of dark matter, couplings to nucleons are indeed isospin violating. Dark matter in the form of a Dirac fermion or complex scalar that is part of a weak doublet will naturally couple in an isospin-violating manner because of the difference in hypercharge of the up and down quarks. This is also the case for dark matter charged under a hidden U(1) gauge group with small kinetic mixing with hypercharge. Likewise, new scalar or fermionic mediators generically couple in a flavor non-universal manner, which can produce isospin-violating couplings to nucleons.

In considering a generic model of dark matter, and in particular a model that could explain the low-mass data, one should really treat the relative coupling to protons and neutrons as a free parameter that can only be determined with guidance from the data. This assumption is sufficient for comparing direct detection experiments, as the relative couplings to protons and neutrons completely define the parameter space. Further assumptions are required when comparing to indirect detection and collider results, and, in particular, assumptions about the flavor structure of the interaction are required since fixing the ratio of proton and neutron cross sections does not uniquely specify the theory. The type of candidate and the mediation mechanism structure also have a significant impact on the comparison between direct detection results and indirect and collider searches.

B. Direct detection

If dark matter interacts with standard model matter through an elastic contact interaction, then the spin-independent differential scattering cross section can be written as

$$\frac{d\sigma}{dE_R} = \frac{\mu_A^2}{M_*^4}[f_p Z + f_n(A-Z)]^2\left[\frac{m_A}{2\mu_A^2 v^2}F^2(E_R)\right], \quad (1)$$

where E_R is the recoil energy, m_A is the mass of the target nucleus, $\mu_A = m_X m_A/(m_X + m_A)$ is the reduced mass, and $F(E_R)$ is a nuclear form factor (assumed to be the same for protons and neutrons). The couplings f_p and f_n parametrize the strengths of dark matter coupling to protons and neutrons, respectively; the interactions are isospin invariant if $f_n = f_p$. The rate of events at a direct detection experiment is thus proportional to the zero-momentum transfer scattering cross section

$$\hat{\sigma}_A = \frac{\mu_A^2}{M_*^4}[f_p Z + f_n(A-Z)]^2, \quad (2)$$

where the proportionality constant is independent of the particle physics model and is determined by the nuclear form factor, the velocity distribution, the target size, and the energy threshold of the experiment.

Direct detection experiments typically report results in terms of σ_N^Z, a "normalized-to-nucleon cross section." This is the nucleon–dark matter scattering cross section that would be inferred, assuming $f_n/f_p = 1$, from the data of a detector using a target with Z protons. For a given isotope with Z protons and A nucleons, the normalized-to-nucleon cross section is related to the dark matter–nucleus zero-momentum transfer cross section by $\sigma_N^Z = (\hat{\sigma}_A/A^2) \times (\mu_p^2/\mu_A^2)$, where μ_p is the dark matter–proton reduced mass.

If dark matter interactions are actually isospin invariant, then σ_N^Z is equal to the proton–dark matter and neutron–dark matter scattering cross sections σ_p and σ_n. For a general ratio of couplings f_n/f_p, σ_N^Z is related to σ_p and σ_n by the "degradation factors" $D_{p,n}^Z$, defined as[1]

$$D_p^Z \equiv \frac{\sigma_N^Z}{\sigma_p} = \frac{\sum_i \eta_i \mu_{A_i}^2 [Z + (f_n/f_p)(A_i - Z)]^2}{\sum_i \eta_i \mu_{A_i}^2 A_i^2}, \quad (3)$$

$$D_n^Z \equiv \frac{\sigma_N^Z}{\sigma_n} = D_p^Z\left(\frac{f_p}{f_n}\right)^2, \quad (4)$$

where the sum is over isotopes i, and η_i is the natural abundance of the ith isotope. If a direct detection experiment uses a target with Z protons, then D_p^Z is the reduction in sensitivity to σ_p relative to the isospin-invariant case, and it rescales the event rate expected for a given value of σ_p. For elements with only one naturally abundant isotope, there exists a choice of f_n/f_p such that $D_{p,n}^Z \to 0$, resulting in zero sensitivity for scattering off those elements. In contrast, if an element has multiple isotopes, there is a lower bound on $D_{p,n}^Z$, since completely destructive interference cannot be simultaneously achieved for all isotopes at once, and there is a reduced but nonzero sensitivity as a worst-case scenario in such elements [14]. An important caveat to these statements is that next-to-leading order (NLO) corrections, including loop corrections and multi-particle exchange, can have a significant effect when the leading order scattering cross section is suppressed [22].

[1]Note, $D_p^Z \equiv 1/F_Z$, where F_Z is defined in Ref. [14].

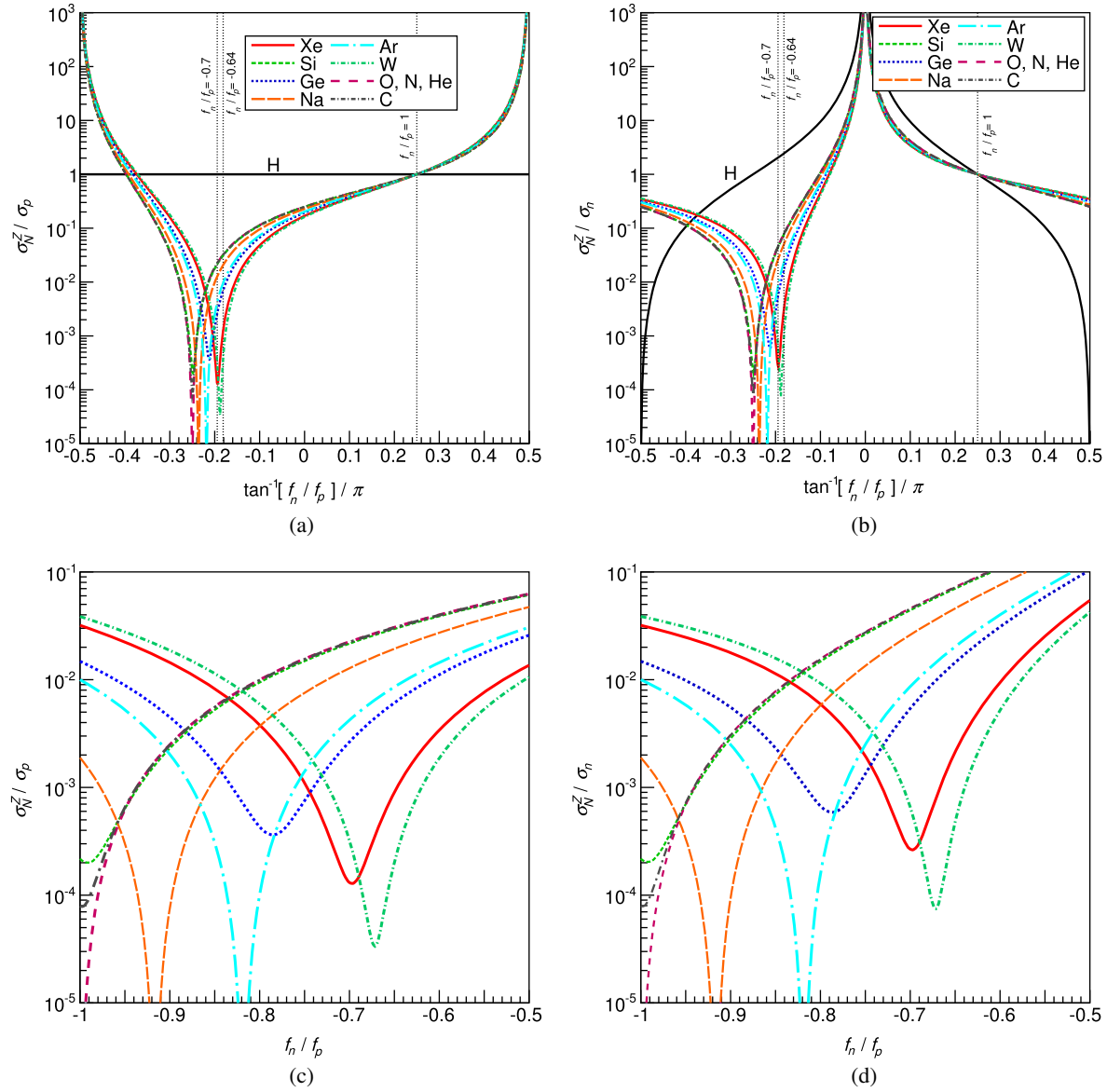

FIG. 2 (color online). Ratio of the normalized-to-nucleon cross section reported by direct detection experiments to the true nucleon cross section. Results are shown for $\sigma_N^Z/\sigma_p = D_p^Z$ (left) and $\sigma_N^Z/\sigma_n = D_n^Z$ (right) as a function of f_n/f_p for various elements. The entire range of f_n/f_p is shown (top) as well as the xenophobic region (bottom). All plots assume $m_X = 8$ GeV, but are highly insensitive to this choice. (a) σ_Z^N/σ_p, entire f_n/f_p range. (b) σ_Z^N/σ_n, entire f_n/f_p range. (c) σ_Z^N/σ_p, xenophobic region. (d) σ_Z^N/σ_n, xenophobic region.

But as the analysis of this effect is model dependent, we will not consider it further. We do note that Ref. [22] found that such effects could either reduce or increase the maximal value of D_p^Z in elements with multiple naturally occurring isotopes.

In Fig. 2 we plot the degradation factors D_p^Z and D_n^Z as a function of f_n/f_p for various elements that are used as targets for low-mass dark matter searches. Generically the sensitivity to σ_p is reduced for $|f_n/f_p| \to 0$ and enhanced for $|f_n/f_p| \to \infty$, with the opposite behavior for sensitivity to σ_n. However, in both cases, sensitivity is significantly reduced for $-1.5 \lesssim f_n/f_p \lesssim -0.5$ by destructive interference. Nearly complete destructive interference occurs for oxygen, nitrogen, helium, sodium, and argon, each of which has only one isotope with significant natural abundance; all other elements have a lower bound on the reduction of sensitivity in the range of 3×10^{-5}–5×10^{-4}.

C. Astrophysical and collider probes

If there is destructive interference between dark matter interactions with protons and neutrons, then the dark matter–proton and dark matter–neutron scattering cross

sections, σ_p and σ_n, must both be larger than σ_N^Z to keep fixed the cross section for dark matter to scatter off the target atomic nucleus (equivalently, $D_{p,n}^Z < 1$). This implies an enhanced coupling to up and down quarks, which in turn implies large potential signals from dark matter annihilation to hadrons and from dark matter production in conjunction with spectator jets or photons at colliders, such as the LHC [23–27].

To consider this possibility concretely, assumptions regarding the type of interaction and couplings to each quark flavor are required. Here we examine the case that dark matter interacts with standard model quarks through a set of effective four-point contact operators. We will consider the set of effective operators that contribute to a spin-independent scattering matrix element (not suppressed by factors of the relative velocity or momentum transfer) and to an S-wave annihilation matrix element. These operators are of interest because they permit unsuppressed spin-independent scattering, which could explain the low-mass direct detection data and also permit S-wave annihilation, which could provide signals at an indirect detection experiment.

If dark matter is a spin-0 particle, then there is a unique such contact operator of dimension 6 or less, $\mathcal{O}_S = (1/M_*)\phi^*\phi\bar{q}q$. If dark matter is a Dirac fermion, there is a different such contact operator, $\mathcal{O}_D = (1/M_*^2)\bar{X}\gamma^\mu X\bar{q}\gamma_\mu q$; there is no such operator if dark matter is a Majorana fermion [28,29]. For either case, if we assume dark matter couples only to up and down quarks, then a choice of f_n/f_p uniquely fixes the relative strength of the dark matter coupling to up and down quarks, and thus uniquely fixes the contact operator up to an overall coefficient. This is a conservative limit of the theory, as including nonzero couplings to heavier quark flavors generically enhances both indirect detection and collider signals, for a fixed direct detection signal.

For a fixed choice of interaction operator and f_n/f_p, one can then translate bounds on the dark matter annihilation cross section from an indirect detection experiment, or bounds on the XX + jet production rate at a collider, into bounds on the overall coefficient of the effective contact operator. This directly corresponds to a bound on the spin-independent scattering cross section.

Assuming dark matter annihilates only to up and down quarks, bounds on the dark matter annihilation cross section [28] were determined from stacked analyses of gamma-ray emissions from dwarf spheroidal galaxies [30,31]. Bounds on σ_p, as a function of f_n/f_p, were then determined in Ref. [28], and we will consider their impact on xenophobic dark matter. There exist systematic uncertainties in the dark matter density profile of the dwarf spheroidals that significantly impact these limits, possibly weakening them by a factor of $\sim$2 or strengthening them by a factor of $\sim$10. Similar bounds can be determined from antiproton searches from Pamela [32–34] or Bess-Polar II [35,36], and have been previously considered in the context of isospin-violating models [37]. However, the systematic uncertainties on these results from propagation models are severe [38], so we focus on the more robust Fermi-LAT dwarf galaxy search.

Collider bounds were produced in Ref. [28] under the same assumption that dark matter couples only to up and down quarks through a contact operator that permits unsuppressed SI-scattering and S-wave annihilation. In that analysis, the number of $pp \to XX$ + jet events expected at the LHC was determined in terms of the overall coefficient of the contact operator. From a comparison of the number of monojet events that passed the cuts to the number expected from standard model background events, bounds on σ_p were determined as a function of f_n/f_p.

Here, we update this analysis using upper bounds on monojet events from new physics at CMS with an integrated luminosity of 4.7 fb^{-1} [39]. Signal events were generated using MadGraph 5.1.5.9 [40] with Pythia 6.4 [41] for showering and Delphes 2.0.5 [42] for detector emulation. The analysis of Ref. [39] provides bounds for monojet $p_T > 110$ GeV and four cuts on missing transverse energy at $\not{E}_T > \{250, 300, 350, 400\}$ GeV. For the Dirac fermion case the strongest limits on $\mathcal{O}_D$ come from the $\not{E}_T > 400$ GeV cut, while for the complex scalar case the strongest limits on $\mathcal{O}_S$ are produced by the $\not{E}_T > 350$ GeV cut. We will also consider the impact of these bounds on models of xenophobic dark matter.

It is important to note, however, that these bounds arising from indirect detection and monojet searches rely on two major assumptions: it is assumed that dark matter interacts through a contact operator even at the energy scales relevant for dark matter annihilation or production, and that this operator permits S-wave annihilation. If dark matter interacts through a true contact operator, then the dark matter scattering, annihilation and production matrix elements all scale as M_*^{-2}, arising from the propagator of the exchanged mediator in the limit where the energy scale of the process is much smaller than the mediator mass. However, if the energy E or momentum transfer scale q of the process is larger than the mediator mass, the matrix element will instead scale as E^{-2} or q^{-2}. This can suppress the dark matter annihilation matrix element ($E \sim 2m_X$) and production matrix element ($E \geq 2m_X$) relative to the scattering matrix element ($E \ll q \sim$ 1–100 MeV). The suppression can be substantial, around $(M_*/m_X)^4$ for mediator masses lighter than the dark matter mass.

If a particular spin-independent direct detection signal is not consistent with the Fermi bounds described here, one implication could be that the interaction cannot be mediated by a contact operator that permits S-wave annihilation; it may instead be permitted by a contact operator that permits P-wave annihilation, or the interaction might not be realizable as a contact interaction at the energy scales relevant for dark matter annihilation. Similarly, if collider

monojet bounds are inconsistent with a particular direct detection signal, the inconsistency could be avoided if the interaction is mediated by an interaction structure that is not a contact interaction at the energy scales of the LHC.

Moreover, the Fermi bounds could also be avoided in the case of asymmetric dark matter [43], wherein the annihilation rate is highly suppressed due to unequal particle and antiparticle species. In such cases indirect detection constraints are effectively removed, but collider constraints remain important.

D. Multiple experiments

For a given experiment the physical quantity σ_p is not truly an observable quantity unless the experiment involves scattering of dark matter off hydrogen—it can only be inferred from σ_N^Z using some assumption regarding the underlying theory. However, one may define the observable ratio

$$R[Z_1, Z_2] \equiv \frac{\sigma_N^{Z_1}}{\sigma_N^{Z_2}} = \frac{D_p^{Z_1}}{D_p^{Z_2}}, \tag{5}$$

which is the ratio of the normalized-to-nucleon scattering cross sections that one would infer for the same dark matter candidate from the data of detectors using two different target materials. A measured dark matter signal at two different experiments (using targets with Z_1 and Z_2 protons, respectively) constitutes an experimental measurement of $R[Z_1, Z_2]$. But as we see from Eq. (4), the equation $D_p^{Z_1} = R[Z_1, Z_2] \times D_p^{Z_2}$ is quadratic in f_n/f_p, with coefficients that are all determined by atomic physics. As a result, with a measurement of $R[Z_1, Z_2]$ from two different experiments with different targets, one can determine f_n/f_p up to a twofold ambiguity.

To illustrate this point, in Fig. 3 we plot the range of σ_p that would be within the silicon- and germanium-based ROIs at $m_X = 8$ GeV as a function of f_n/f_p. We also plot exclusion contours from XENON100, from Fermi, and from CMS monojet searches. For the Fermi and CMS monojet search bounds, it is assumed that dark matter is either a complex scalar or Dirac fermion that interacts through a contact operator permitting S-wave annihilation and spin-independent scattering with no momentum or velocity suppression. If dark matter is a real scalar, then the Fermi-LAT bounds would be stronger than in the complex scalar case by a factor of 2, while the CMS monojet bounds would be weaker by a factor of 2 [28].

In particular, one sees that the σ_p ROI corresponding to CDMS-Si overlaps the germanium-based CoGeNT and CDMS ROIs for a wide range of the parameter f_n/f_p, which includes the isospin-invariant case $f_n/f_p = 1$. But there is another narrow region, $f_n/f_p = -0.89 \pm 0.05$, for which the CDMS-Si and germanium-based ROIs also overlap. It is clear however that XENON100's sensitivity relative to silicon- or germanium-based experiments is enhanced in this second region, producing complete exclusion. Moreover, although Fermi would not probe models that could match the silicon-based and germanium-based

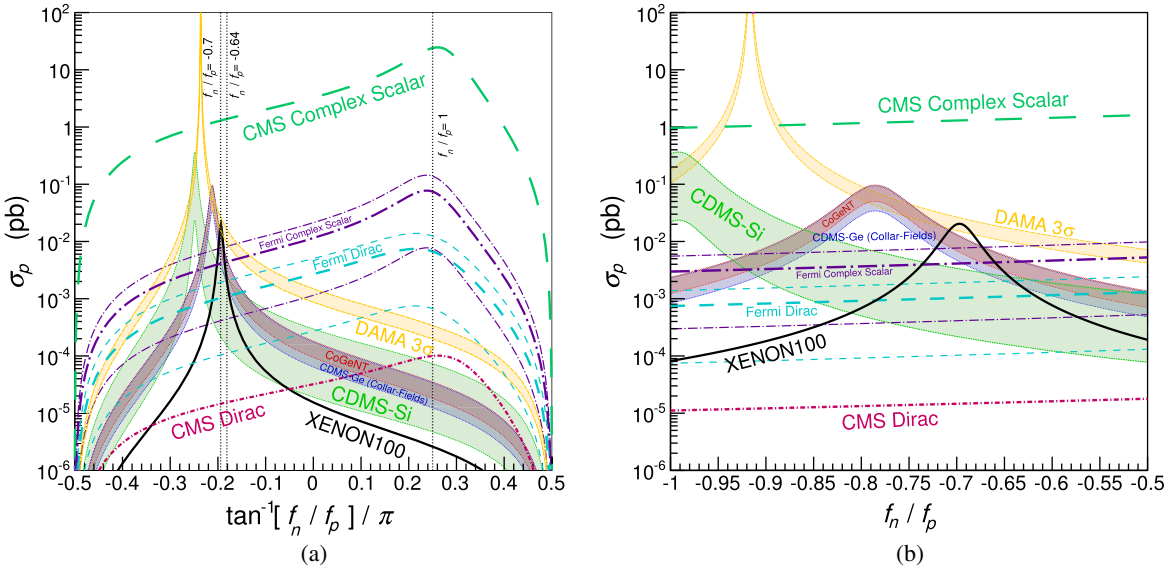

FIG. 3 (color online). Proton cross section for various experiments as a function of f_n/f_p for $m_X = 8$ GeV. Plotted are slices of the 90% CL ROIs for CDMS-Si [4], CoGeNT [19], and CDMS-Ge (Collar/Fields) [20], the 3σ ROI for DAMA [1], and exclusion contours for XENON100 [6]. Also plotted are 90% CL exclusion contours for CMS [39] and for the Fermi-LAT [31], assuming dark matter is either a complex scalar or Dirac fermion coupling only to first generation quarks through an effective contact interaction permitting unsuppressed spin-independent scattering and S-wave annihilation. The thin dot-dashed violet and dashed teal lines correspond to the systematic uncertainty in the Fermi-LAT bounds from astrophysical uncertainties for complex scalar and Dirac fermion candidates, respectively. (a) Entire f_n/f_p range. (b) Xenophobic region.

ROIs for $f_n/f_p = 1$, it rules out models that could match these regions for $f_n/f_p \approx -0.89$, if dark matter interacts through a contact interaction yielding S-wave annihilation. Finally, we see from Fig. 3 that the silicon- and germanium-based ROIs overlap yet again for $f_n/f_p \ll -1$. The appearance of a third overlap region may seem surprising since f_n/f_p is determined by a quadratic equation. But this result is readily understood from the fact that the current regions of interest are of finite size. Since the silicon- and germanium-based ROIs are broad enough to be consistent for $f_p \approx 0$, it is not surprising that the ROIs overlap for both $f_n/f_p \gg 1$ and $f_n/f_p \ll -1$. With greater exposure of the detectors, the bands corresponding to these ROIs should become thinner. One can see from Fig. 3 that either of the overlap regions at $f_n/f_p \sim 1$ or $f_n/f_p < -1$ could then disappear; indeed, one of these solutions would necessarily go away. However, the solution with $f_n/f_p \approx -0.89$ is robust.

Although we have studied IVDM in the context of the particular details of current low-mass data, the points we have made are quite generic. In general, experimental signals of dark matter from two different direct detection experiments can determine f_n/f_p up to a twofold ambiguity, which can be resolved by a detection or exclusion from a third detector, and potentially by signals from indirect detection or collider monojet searches. The finite width of the ROIs supplements need for at least three independent signals to determine f_n/f_p.

III. XENOPHOBIC DARK MATTER

In the current generation of direct detection experiments the reported sensitivity of XENON100 [5,6] exceeds that of all others by at least an order of magnitude, and the results from the LUX experiment [21] are expected to exceed that sensitivity significantly within the year. From Fig. 3, it is apparent that dark matter is maximally xenophobic for $f_n/f_p \approx -0.70$ and the coupling significantly suppressed for nearby values; however, for that value the current silicon-based and germanium-based ROIs do not overlap. On the other hand, for slightly less xenophobic dark matter, $f_n/f_p \approx -0.64$, the 90% CL silicon- and germanium-based ROIs have a region of overlap that is marginally consistent with exclusion contours from XENON100. For this choice of f_n/f_p, we plot in Fig. 1(c) the silicon- and germanium-based ROIs, and XENON100, Fermi and CMS monojet exclusion contours as a function of m_X, along with projected limits from LUX. We thus see that, though this region of parameter space can potentially reconcile the current germanium-, silicon-, and xenon-based detector data, it can be decisively probed if data from LUX significantly improves upon XENON100's current sensitivity. The current projected sensitivity at LUX does not conclusively probe the disputed region, and indeed the LUX experiment claims no sensitivity to dark matter with $m_X \lesssim 7$ GeV; however, the LUX Collaboration uses very conservative estimates for their light collection efficiency, and a dedicated ionization-only analysis could still produce sensitivity to the low-mass region [44].

It is interesting to note that this model is in tension with both collider and Fermi bounds if dark matter is a Dirac fermion interacting through a contact operator that permits S-wave annihilation. However, if dark matter is a complex scalar that couples through an effective contact operator permitting S-wave annihilation, then this model is

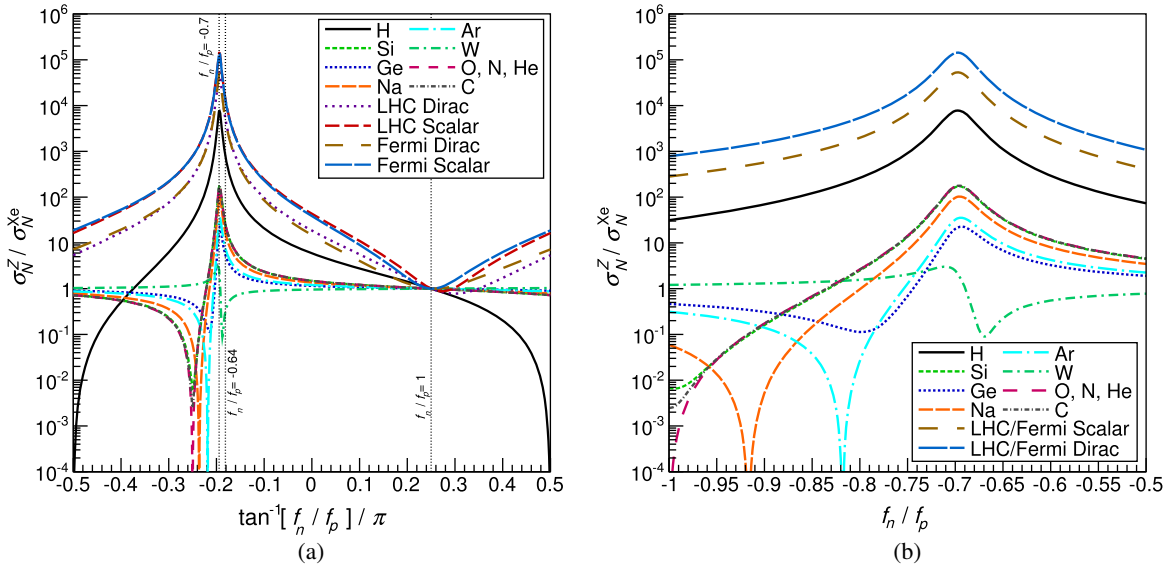

FIG. 4 (color online). Ratio of σ_N^Z in various experiments to σ_N^{Xe}. Results are shown as a function of f_n/f_p for scattering off various elements, as well as for LHC and Fermi determinations. In the xenophobic region the behavior of LHC and Fermi bounds for a given operator are visually identical. (a) Entire f_n/f_p range. (b) Xenophobic region.

consistent with collider bounds, but only marginally consistent with bounds from Fermi searches of dwarf spheroidal galaxies. In particular, systematic uncertainties in the dark matter density profile of the dwarf spheroidals can have a large impact on the consistency of the Fermi data with this model. This suggests that any future results from Fermi, positive or negative, could have an interesting impact on this scenario. If indeed the data are explained by a model in which dark matter is a xenophobic complex scalar interacting through an effective contact operator, then one should expect that Fermi will soon see an excess of gamma rays from dwarf spheroidal galaxies. If Fermi does not see such an excess, this suggests that a model of this type can only be consistent with the data if the interaction is not a contact interaction. If dark matter interacts through a contact operator that only permits P-wave annihilation, then although the Fermi bounds would be satisfied, the bounds from collider searches would become problematic.

The overall enhancement of various experimental signals relative to xenon-based detectors is shown in Fig. 4. Although $D_p^{\mathrm{Xe}} \sim 10^{-4}$ at its minimum, as shown in Fig. 2, D_p^Z is also suppressed for all elements except hydrogen in the range $-1.5 \lesssim f_n/f_p \lesssim -0.5$. As a result, the maximal value of $R[Z, \mathrm{Xe}]$ ranges from $\sim$20 to $\sim$200 for various lighter elements relevant for direct detection. In contrast, collider and annihilation signals suffer no suppression in this region and are even enhanced relative to scattering off protons, resulting in a maximal $R[\{\mathrm{LHC, annihilation}\}, \mathrm{Xe}]$ of $\sim 10^5$.[2] It is also worth noting that, as one moves away from the maximally xenophobic limit, one would expect NLO corrections to the scattering cross section to be less important.

IV. CONCLUSIONS

We have revisited the discussion of isospin-violating dark matter as a way of potentially reconciling several recent positive signals at low mass from direct detection experiments with very tight exclusion contours from xenon-based detectors. Our focus has been on xenophobic dark matter: dark matter in which destructive interference between coupling to protons and neutrons drastically reduces the sensitivity of xenon-based detectors. We note, importantly, that the large natural abundance of several xenon isotopes implies that even xenophobia has its limits [14]; there is no choice of parameters that can completely eliminate the response of all xenon isotopes.

Focusing on recent positive signals from CDMS-Si detectors and the CoGeNT experiment, and on a ROI identified by an analysis of CDMS-Ge detectors from Collar and Fields, we have found that these ROIs can potentially be made to overlap in a region marginally consistent with bounds from XENON100 for dark matter that is near maximally xenophobic, with $f_n/f_p \approx -0.64$. While a true global likelihood analysis to determine if this region is a good fit to the combined data is beyond the scope of this work, even in this prescription the improvement in consistency is qualitatively clear.

Moreover, we have only focused on the effect of isospin violation; changes to astrophysics assumptions can alter this picture, possibly producing more alignment of current results. New results will also alter the picture, in particular new data from CoGeNT that may result in refining their ROI. More generally, we have shown that the results from multiple detectors and from independent detection strategies, such as indirect or collider searches, provide important complementary data, which are necessary for clarifying the consistency of the low-mass data. In particular, new results from LUX and from Fermi dwarf spheroidal searches should provide important tools for testing models of xenophobic dark matter.

This analysis highlights the importance of improvements in direct detection experiments for clarifying the viability of models of low-mass dark matter. In particular, even though it is a xenon detector, LUX may have much to say about the xenophobic models discussed here. This hinges critically on LUX's sensitivity to $\sim$8 GeV dark matter, which will depend in detail on the charge and light yields of liquid xenon (as well as the backgrounds) at low recoil energies. LUX may be capable of achieving a low-mass sensitivity significantly greater than the estimates used here, but such an assessment must likely await a full analysis of the data.

ACKNOWLEDGMENTS

We are grateful to E. Figueroa and D. McKinsey for useful discussions. We are grateful to the organizers of the APS April Meeting, to the organizers of the Light Dark Matter Workshop at MCTP, and to the KITP, where part of this work was conducted. The work of J. L. F. is supported in part by NSF Grant No. PHY–0970173 and a Simons Foundation Fellowship. The work of J. K. prior to June 1, 2013 was supported in part by U.S. Department of Energy Grant No. DE–FG02–04ER41291. D. S. is supported in part by U.S. Department of Energy Grant No. DE–FG02–92ER40701 and by the Gordon and Betty Moore Foundation through Grant No. 776 to the Caltech Moore Center for Theoretical Cosmology and Physics.

[2] $R[\{\mathrm{LHC, annihilation}\}, \mathrm{Xe}] \equiv \sigma_N^{\{\mathrm{LHC,annihilation}\}}/\sigma_N^{\mathrm{Xe}}$, where $\sigma_N^{\{\mathrm{LHC,annihilation}\}}$ is the dark matter–nucleon scattering cross section that would be inferred from LHC/indirect detection data if one assumed $f_n/f_p = 1$.

[1] R. Bernabei *et al.* (DAMA and LIBRA Collaborations), Eur. Phys. J. C **67**, 39 (2010).
[2] C. Aalseth *et al.* (CoGeNT Collaboration), Phys. Rev. Lett. **106**, 131301 (2011).
[3] G. Angloher, M. Bauer, I. Bavykina, A. Bento, C. Bucci *et al.*, Eur. Phys. J. C **72**, 1971 (2012).
[4] R. Agnese *et al.* (CDMS Collaboration), arXiv:1304.4279 [Phys. Rev. Lett. (to be published)].
[5] E. Aprile *et al.* (XENON Collaboration), Phys. Rev. Lett. **107**, 131302 (2011).
[6] E. Aprile *et al.* (XENON100 Collaboration), Phys. Rev. Lett. **109**, 181301 (2012).
[7] M. T. Frandsen, F. Kahlhoefer, C. McCabe, S. Sarkar, and K. Schmidt-Hoberg, arXiv:1304.6066.
[8] Y.-Y. Mao, L. E. Strigari, and R. H. Wechsler, arXiv:1304.6401.
[9] R. C. Cotta, A. Rajaraman, T. M. P. Tait, and A. M. Wijangco, arXiv:1305.6609.
[10] A. Kurylov and M. Kamionkowski, Phys. Rev. D **69**, 063503 (2004).
[11] F. Giuliani, Phys. Rev. Lett. **95**, 101301 (2005).
[12] S. Chang, J. Liu, A. Pierce, N. Weiner, and I. Yavin, J. Cosmol. Astropart. Phys. 08 (2010) 018.
[13] Z. Kang, T. Li, T. Liu, C. Tong, and J. M. Yang, J. Cosmol. Astropart. Phys. 01 (2011) 028.
[14] J. L. Feng, J. Kumar, D. Marfatia, and D. Sanford, Phys. Lett. B **703**, 124 (2011).
[15] J. Angle *et al.* (XENON10 Collaboration), Phys. Rev. Lett. **107**, 051301 (2011).
[16] D. Akerib *et al.* (CDMS Collaboration), Phys. Rev. D **82**, 122004 (2010).
[17] Z. Ahmed *et al.* (CDMS-II Collaboration), Phys. Rev. Lett. **106**, 131302 (2011).
[18] C. Aalseth *et al.* (CoGeNT Collaboration), arXiv:1208.5737.
[19] C. Kelso, D. Hooper, and M. R. Buckley, Phys. Rev. D **85**, 043515 (2012).
[20] J. Collar and N. Fields, arXiv:1204.3559.
[21] D. Akerib *et al.* (LUX Collaboration), Astropart. Phys. **45**, 34 (2013).
[22] V. Cirigliano, M. L. Graesser, and G. Ovanesyan, J. High Energy Phys. 10 (2012) 025.
[23] A. Birkedal, K. Matchev, and M. Perelstein, Phys. Rev. D **70**, 077701 (2004).
[24] J. L. Feng, S. Su, and F. Takayama, Phys. Rev. Lett. **96**, 151802 (2006).
[25] M. Beltran, D. Hooper, E. W. Kolb, Z. A. Krusberg, and T. M. Tait, J. High Energy Phys. 09 (2010) 037.
[26] J. Goodman, M. Ibe, A. Rajaraman, W. Shepherd, T. M. P. Tait, and H.-B. Yu, Phys. Lett. B **695**, 185 (2011).
[27] P. J. Fox, R. Harnik, J. Kopp, and Y. Tsai, Phys. Rev. D **85**, 056011 (2012).
[28] J. Kumar, D. Sanford, and L. E. Strigari, Phys. Rev. D **85**, 081301 (2012).
[29] J. Kumar and D. Marfatia, arXiv:1305.1611.
[30] M. Ackermann *et al.* (Fermi-LAT Collaboration), Phys. Rev. Lett. **107**, 241302 (2011).
[31] A. Geringer-Sameth and S. M. Koushiappas, Phys. Rev. Lett. **107**, 241303 (2011).
[32] O. Adriani *et al.* (PAMELA Collaboration), Phys. Rev. Lett. **106**, 201101 (2011).
[33] Q.-H. Cao, I. Low, and G. Shaughnessy, Phys. Lett. B **691**, 73 (2010).
[34] J. Lavalle, Phys. Rev. D **82**, 081302 (2010).
[35] K. Abe, H. Fuke, S. Haino, T. Hams, M. Hasegawa *et al.*, Phys. Rev. Lett. **108**, 051102 (2012).
[36] R. Kappl and M. W. Winkler, Phys. Rev. D **85**, 123522 (2012).
[37] H.-B. Jin, S. Miao, and Y.-F. Zhou, Phys. Rev. D **87**, 016012 (2013).
[38] C. Evoli, I. Cholis, D. Grasso, L. Maccione, and P. Ullio, Phys. Rev. D **85**, 123511 (2012).
[39] S. Chatrchyan *et al.* (CMS Collaboration), J. High Energy Phys. 09 (2012) 094.
[40] J. Alwall, M. Herquet, F. Maltoni, O. Mattelaer, and T. Stelzer, J. High Energy Phys. 06 (2011) 128.
[41] T. Sjostrand, S. Mrenna, and P. Z. Skands, J. High Energy Phys. 05 (2006) 026.
[42] S. Ovyn, X. Rouby, and V. Lemaitre, arXiv:0903.2225.
[43] N. Okada and O. Seto, arXiv:1304.6791.
[44] D. Hooper, arXiv:1306.1790.
[45] C. Savage, G. Gelmini, P. Gondolo, and K. Freese, J. Cosmol. Astropart. Phys. 04 (2009) 010.
[46] C. Savage, G. Gelmini, P. Gondolo, and K. Freese, Phys. Rev. D **83**, 055002 (2011).
[47] E. Armengaud *et al.* (EDELWEISS Collaboration), Phys. Rev. D **86**, 051701 (2012).
[48] H. Li *et al.* (TEXONO Collaboration), arXiv:1303.0925.
[49] W. Zhao *et al.* (CDEX Collaboration), arXiv:1306.4135.